Letters in High Energy Physics
ISSN: 2632-2714
Volume 2024

Emission of Oblique Propagating Electromagnetic Ion Cyclotron Waves through Hot Injection of Ion Beams for Ring Distribution with A.C. Electric Field in the Jovian Magnetosphere

[1]Garima Yadav , [1]B.S.Sharma, [2]Ankita and [3]Sanjeet Kumar

[1]Department of Physics ,Lords University,Alwar-301001,India

[2]Department of Physics, Amity Institute of Applied Sciences, Amity University, Sector – 125 Noida, Uttar Pradesh, India

3 PG Department of Physics, HD Jain College, Veer Kunwar Singh University, Ara, Bhojpur, Bihar, India.

Garima Yadav, 1241@s.lordsuni.edu.in , ORCID iD-https:orcid.org/0009-0005-3239-5996

B.S.Sharma, bssharma@lordsuni.edu.in, ORCID iD-https:orcid.org/0000-0002-2327-9396

Corresponding author -Ankita, ankitac@amity.edu, ORCID iD- https://orcid.org/0009-0009-2201-6453

Sanjeet Kumar E-mail address, san.phy18@gmail.com

Abstract

The Ulysses spacecraft's detection of electromagnetic ion-cyclotron waves in the Jovian magnetosphere is examined in this research. In this area, several kinds of high-frequency radio emissions from resonant interactions have been detected. In light of the parallel propagation of electromagnetic ion-cyclotron waves, the study focuses on the wave-particle interactions between these waves and fully ionized magnetospheric plasma particles. As a result, the dispersion relation with a ring distribution in a collisionless magneto-plasma at 17 RJ with a parallel alternating current (AC) electric field may be thoroughly examined. We derive a relativistic growth rate expression using a kinetic approach and a method of characteristics. We also examine injection events captured in the Jovian magnetosphere by the Galileo spacecraft's energetic particle detector (EPD). We perform a parametric analysis of different plasma properties, including temperature anisotropy, AC frequency, and relativistic variables, after a hot ion beam is injected to investigate their impact on the growth rate, which is displayed.

Keywords- Oblique Electromagnetic ion-cyclotron waves, Ring distribution, hot ion injection, Jovian magnetosphere

Introduction

The electromagnetic ion cyclotron (EMIC) wave is typically a left-handed polarized transverse wave, generated when the perpendicular ion temperature ($T_\perp$) exceeds the parallel temperature ($T_\parallel$), with ion temperatures in the range of 10–100 keV [1]. EMIC waves are thought to originate near the magnetic equator, where the magnetic field strength is minimal along a given field line, and subsequently propagate along the field lines toward higher latitudes [2,3]. In Earth's magnetosphere, EMIC waves are categorized into three distinct frequency bands based on the gyrofrequencies of dominant ion species: the Hydrogen band (H-band), between the gyrofrequencies of H+ and He+ ions; the Helium band (He-band), between the gyrofrequencies of He+ and O+ ions; and the Oxygen band (O-band), which occurs at frequencies below the gyrofrequency of O+ ions[4,5] .

These waves play a significant role in wave-particle interactions and can lead to ion scattering, which is particularly relevant for radiation belt dynamics and plasma heating in planetary magnetospheres [6.7]. Recent studies have also highlighted the generation and propagation mechanisms of EMIC waves in other planetary magnetospheres, such as those of Jupiter and Saturn, where similar wave phenomena are observed [8,9,10].

Previous research has demonstrated that electromagnetic ion cyclotron (EMIC) waves can interact with both energetic ions non relativistic and relativistic electrons [11,12]. Through wave-particle

interactions, particles can be scattered into the loss cone, leading to their precipitation into the upper atmosphere. Furthermore, observational studies have shown that EMIC waves can induce heating of He+ ions as well as electrons [13]. These interactions are crucial for the energization of cold plasma particles and the loss of high-energy relativistic particles within the magnetosphere[3].

Jupiter, the largest planet in our solar system, is a gas giant with distinct properties that make it a prime target for scientific investigation. Named after the king of the Roman gods, Jupiter has intrigued astronomers and space scientists for centuries (NASA Solar System Exploration: Jupiter). Its magnetosphere is a vast and powerful region shaped by the planet's rapid rotation, metallic hydrogen core, and interactions with the solar wind [14] This magnetic environment is primarily driven by Jupiter's fast rotational period, the metallic hydrogen within its interior, and the extensive influence of its large moon system.

Numerous studies have identified various sources that contribute to the generation of EMIC waves in different regions of the magnetosphere. EMIC waves observed in the post-noon to dusk sector, for example, are primarily generated by energetic ions within the current ring region [8]. In this sector, the thermal anisotropy of these high-energy particles plays a critical role in the generation of EMIC waves. Additionally, it has been shown that the high density of cold plasma within the plasmasphere diminishes the resonant strength of the energetic ions, thereby influencing the efficiency of wave generation. These findings suggest that the optimal region for EMIC wave production is where the energetic ion rings intersect with the cold ions of the plasmasphere [15,16,17,18]. Furthermore, cold plasma condensation and the formation of cold ions have been identified as key mechanisms influencing the structure and generation of EMIC waves [17]. Beyond the current rings, the presence of ion sheets in the outer magnetosphere also plays a significant role in modulating EMIC wave emissions [8,19].

Numerous studies have identified that the primary source regions of EMIC waves under geomagnetic disturbances (such as magnetic storms and substorms) are associated with the injection and concentration of cold plasma within the magnetosphere. To explore the spatial distribution of EMIC waves in relation to geomagnetic activity, several studies have correlated wave occurrence with geomagnetic indices such as AE (Auroral Electrojet index), SYM-H (symmetrical component of the horizontal geomagnetic field), and Kp (planetary K-index). However, research examining the correlation of EMIC wave properties with geomagnetic indices (SYM-H, AE, and Kp) using observations from the Combined Release and Radiation Effects Satellite (CRRES) has shown that these indices do not provide a reliable means of determining the specific characteristics of EMIC waves. These findings suggest that distinguishing internal wave sources from external sources is challenging when relying solely on geomagnetic indices [20].

Recent observations by the Juno spacecraft have revealed a new class of broadband plasma wave emissions (~50 Hz to 40 kHz) detected on 27 August 2016, as the spacecraft passed over Jupiter's low-altitude polar regions. Large-amplitude electromagnetic waves were simultaneously detected with intense electron fluxes precipitating along auroral field lines at Jupiter. These observations support the idea that counter-streaming electron beams drifting along the magnetic field in electron–proton plasmas can generate electrostatic (ES) waves and structures commonly observed in planetary magnetospheres. In electron–positron plasmas, streaming electron/positron beams along the magnetic field can initially produce ES waves, followed by the generation of electromagnetic (EM) waves with significant magnetic field perturbations [21,22].

This paper aims to investigate the effect of hot ion injection on electromagnetic ion cyclotron (EMIC) wave instability in the Jovian magnetosphere, drawing parallels with cold beam injection studies for whistler wave generation in Saturn's magnetosphere [23]. Plasma injection processes and energy exchange play a crucial role in the dynamics of Jupiter's magnetosphere. A detailed derivation of the dispersion relation for EMIC waves is presented, considering a ring distribution in the presence of a parallel AC electric field. Additionally, an expression for the growth rate of EMIC waves is derived in terms of temperature anisotropy and the electric field in an anisotropic plasma. Finally, the growth rate for EMIC waves under Jovian magnetospheric conditions at L = 17 R_J is calculated, and the results are discussed. This

analysis will contribute to a deeper understanding of the physical mechanisms behind the various broadband emissions observed in Jupiter's magnetosphere and ionosphere [24,25,26].

Dispersion relation and Growth rate

A spatially homogeneous, collisionless, and anisotropic plasma is assumed, aligned with the z-direction of the ambient magnetic field **B** and an external alternating current (AC) electric field. This configuration is used to derive the dispersion relation, while accounting for small inhomogeneities within the interaction zone. The Vlasov-Maxwell equations are employed, and after separating the equilibrium and non-equilibrium components, higher-order terms are neglected. This approach follows the methodology and geometric considerations outlined of [27], as well as similar techniques used in previous studies of plasma wave interactions in magnetospheres. The assumptions and simplifications are consistent with the treatments of wave-plasma interactions in anisotropic plasmas discussed , where similar configurations of AC electric fields and magnetic field alignments have been considered from [28,29,30].

The dispersion relation for relativistic case with parallel AC electric field is written from Garima et al[31] of equations (1) and (2) for n=1as:

$$\frac{k^2c^2\cos\theta}{\omega^2} = 1 + \sum_s \frac{4e_s^2\pi}{(\beta m_s)^2\omega^2}\sum J_p(\lambda_2)\int \frac{d^3p}{2} p_\perp \begin{bmatrix} (\beta m_s)\left(\omega - \frac{k_{||}p_{||}}{\beta m_s}\right)\frac{\partial f_o}{\partial p_\perp} \\ -k_{||}(\beta m_s)\frac{\partial f_o}{\partial p_\perp}\frac{\Gamma_z}{\beta\nu}\left(\frac{p}{\lambda_2}-1\right) \\ +k_{||}p_\perp\frac{\partial f_o}{\partial p_{||}} \end{bmatrix}\left(\frac{1}{\omega - \frac{k_{||}p_{||}}{\beta m_s} - \frac{k_{||}\Gamma_z}{\beta\nu} + pv \pm \frac{\omega_c}{\beta}}\right) \quad ...(1)$$

where, subscript 's' denotes type of species i.e. electrons and ions. where, β is the relativistic factor and defined as $= 1/\sqrt{1-\frac{v^2}{c^2}}$. For propagation of electromagnetic wave

The ring distribution function is assumed to be distribution function of the trapped particles from [30,32]

$$f(p_\perp, p_{||}) = \frac{n_s/n}{\pi^{3/2}p_{o||s}p_{o\perp s}^2 A}\exp\left[-\frac{(p_\perp - v_o)^2}{p_{o\perp s}^2} - \frac{(p_{||}^2)}{p_{o||s}^2}\right] \quad \ldots(2)$$

$$A = \exp\left(-\frac{v_o^2}{p_{o\perp s}^2}\right) + \sqrt{\pi}\left(\frac{v_o}{p_{o\perp s}}\right)\mathrm{erfc}\left(-\frac{v_o}{p_{o||s}}\right) \quad \ldots(3)$$

$p_{o||e} = \left(k_b T_{||e}/\beta m_e\right)^{1/2}$, $p_{o\perp e} = (k_b T_\perp/\beta m_e)^{1/2}$, $p_{o||i} = \left(k_b T_{||i}/\beta m_i\right)^{1/2}$ and $p_{o\perp i} = (k_b T_{\perp i}/\beta m_i)^{1/2}$ are the associated parallel and perpendicular thermal momenta of ions and electrons.

For oblique propagation of electromagnetic ion-cyclotron wave, the general dispersion relation reduces to $\varepsilon_{11} \pm i\varepsilon_{12} = N^2\cos^2\theta$

n_s/n in equation (2) represents the ratio of particle total density captured and characterized by high energy, and erfc(x) in equation (3) is a complementary error function. The drift velocity is represented as v_o.

Substituting $d^3p = 2\pi\int_0^\infty p_\perp \mathrm{d}p_\perp \int_{-\infty}^\infty \mathrm{d}p_{||}$ and using expression (2) in equation (1) and after solving the integrations, we get the dispersion relation as:

$$\frac{k^2c^2\cos\theta}{\omega^2} = 1 + \frac{4e_s^2\pi}{(\beta m_s)^2\omega^2}\sum_p J_p(\lambda_2)\frac{(n_s/n)}{A}(\beta m_s)\left[\frac{\beta m_s}{p_{o||s}}\left(\frac{\omega}{k_{||}} - \frac{\Gamma_{||s}}{\beta\nu}\left(\frac{p}{\lambda_2}-1\right)\right)X_1 Z(\xi) + X_2\left(1 + \xi Z(\xi)\right)\right] \quad \ldots(4)$$

The above dispersion relation is now approximated in ion cyclotron range of frequencies. In this case electrons temperature $T_{\wedge e} = T_{\|e} = T_e$ are assumed and magnetized with $\left|w_r + ig\right| << w_{ci}$whereas ions are assumed to have the condition $T_{\wedge i} > T_{\|i}$ and $\left|k_{\|}a_{\|i}\right| << \left|w_r \pm w_{ci} + ig\right|$. So, considering these approximations, equation (4) becomes:

$$D(k,\omega_r+i\gamma)=1-\frac{k^2c^2}{(\omega_r+i\gamma)^2}+\sum_p J_p(\lambda_2)\left[\begin{array}{c}\left(\frac{\omega_{pe}^2}{\omega_{ci}^2}-\frac{\omega_{pe}^2}{(\omega_r+i\gamma)(\pm\omega_{ci})}\right)X_{1e}(\beta m_e)\\ +\frac{\omega_{pi}^2}{(\omega_r+i\gamma)^2}\left(\begin{array}{c}X_{1i}\frac{(\beta m_i)}{p_{o||i}}\left(\frac{\omega_r+i\gamma}{k_{||}}-\frac{\Gamma_{||i}}{\beta\nu}\left(\frac{p}{\lambda_2}-1\right)\right)Z(\xi_i)\\ +X_{2i}\left(1+\xi_i Z(\xi_i)\right)\end{array}\right)\end{array}\right] \quad \ldots(5)$$

Where,

$X_{1i}=1+\frac{v_o^2}{p_{o\perp i}^2}-\sqrt{\pi}\frac{v_o}{p_{o\perp i}}$,

$X_{1e}=1+\frac{v_o^2}{p_{o\perp e}^2}-\sqrt{\pi}\frac{v_o}{p_{o\perp e}}$ and

$X_{2i}=X_{1i}+\frac{p_{o\perp i}^2}{p_{o||i}^2}\left(1-\sqrt{\pi}\frac{v_o^3}{p_{o\perp i}^3}erfc\left(\frac{v'_{\perp i}}{p_{o\perp i}}\right)+3\frac{v_o^2}{p_{o\perp i}^2}-\frac{3}{2}\sqrt{\pi}\frac{v_o}{p_{o\perp i}}\right)$

After applying the condition of charge neutrality $\frac{W_{pe}^2}{\pm W_{ce}^2}=\frac{-W_{pi}^2}{\pm W_{ci}^2}$ and the another condition $\left|\frac{k^2c^2}{W^2}>>1+\frac{W_{pe}^2}{W_{ce}^2}\right|$

, the dispersion relation reduces to

$$D(k,\omega_r+i\gamma)=-\frac{k_{||}^2c^2}{\omega_{pi}^2}\cos\theta+\sum_p J_p(\lambda_2)\left[\begin{array}{c}\frac{\omega}{\pm\omega_{ci}}(\beta m_e)X_{1e}\\ +(\beta m_i)X_{1i}\left\{\frac{\beta m_i}{p_{o||i}}\left(\frac{\omega}{k_{||}}-\frac{\Gamma_{||i}}{\beta\nu}\left(\frac{p}{\lambda_2}-1\right)\right)Z(\xi_i)+\frac{X_{2i}}{X_{1i}}\left(1+\xi_i Z(\xi_i)\right)\right\}\end{array}\right]$$

…(6)

The function of plasma dispersion is given by$Z(\xi)=\frac{1}{\sqrt{\pi}}\int_{-\infty}^{\infty}\frac{e^{-t^2}}{t-\xi}$dt,

Where $\xi=\frac{\beta m_i\omega-\frac{k_{||}\Gamma_{||s}m_i}{\nu}+(\beta m_i)p\nu\pm m_i\omega_c}{k_{||}p_{o||i}}$

$\omega_{pi}^2=\frac{4\pi e^2}{(\beta m_i)^2}\frac{n_i/n}{B}$

Now, dimensionless parameter wave vector $\tilde{k}=\frac{k_{||}p_{o||i}}{\omega_{ci}}$ is introduced. The expression for dimensionless growth rate by using standered formula can be written for oblique propagation of EMIC wave as

$$\frac{\gamma}{\omega_{ci}}=\frac{\frac{\sqrt{\pi}}{\tilde{k}\cos\theta_1}\left(\frac{X_{2i}}{X_{1i}}-k_4\right)k_3^3\exp\left[-\left(\frac{k_3^2}{\tilde{k}\cos\theta}\right)^2\right]}{1+\frac{\tilde{k}^2\cos\theta_1^2}{2k_3^2}+\frac{\tilde{k}^2\cos\theta_1^2}{k_3}\left(\frac{X_{2i}}{X_{1i}}-k_4\right)+\frac{m_eX_{1e}}{m_iX_{1i}}k_3^2}$$

$X_3=-\frac{\beta\omega_r}{\omega_c}=X_4+\frac{\tilde{k}^2\cos\theta_1^2}{2\beta_1}\left[\frac{X_{2i}}{X_{1i}}\frac{\beta_1}{(1+X_4)}-\frac{(1+X_4)}{\beta X_{1i}}\right]$

Where $k_3=1-\beta X_3+\beta X_4$, $k_4=\frac{\beta X_3-\beta X_4}{1-\beta X_3+\beta X_4}$ and $b_1=\frac{4\pi m_o e_o k_b T_{||i}\left(n_i/n\right)}{AB_o^2}$ where θ_1 is propogation angle

$X_4=\frac{k_{||}\Gamma_{||i}}{\beta\nu\omega_c}-\frac{p\nu}{\omega_c}$

The above expresssion has been used for beam and background plasma to analyze the effect of hot injected ion beam on EMIC waves.

Magnetic field model used is taken from Agarwal et al.,[33]

$$B = B_0\left(\frac{[1+3\,sin^2\,\theta]^{\frac{1}{2}}}{cos^6\,\theta}\right)$$

where,

B_0 is magnetic field at equator and

θ represents the magnetic latitude.

Plasma Parameters

In their study, [33] reported injection events observed by the Galileo spacecraft within Jupiter's magnetosphere, specifically between radial distances of 9 and 27 Jovian radii (R_J), for energetic particles with energies exceeding 20 keV. To assess the effect of hot ion injection on electromagnetic ion cyclotron (EMIC) wave growth within the Jovian magnetosphere, a set of background plasma parameters was considered at a radial distance of R ~ 17 R_J, where the background magnetic field strength is approximately B_o = 51 nT, p=1 Kivelson and Khurana, [34]. The key plasma parameters include a cold ion number density of , with a temperature anisotropy of A_T = 1.5, and propagation angle for oblique propagation, θ_1 =10° ion and electron thermal energies of $K_BT_{\|i}$ =1 keV and $K_BT_{\|e}$ =200eV respectively. Upon injecting warm plasma, the following parameters were adopted for the warm ion distribution: a number density of $n_w = 3 \times 10^7$ m^{-3}, with varying temperature anisotropies A_T=1.75, 2, 2.25, thermal energy of ions and electrons $K_BT_{\|i}$ =3 keV and $K_BT_{\|e}$ =200eV. The ratio of cold to warm ion number densities was set at n_c/n_w=1/10. According to previous studies, the approximate magnitudes of the electric and magnetic fields in this region were taken to be E ≈ 10 mV/m and B ≈ 51 nT, and latitude, θ =10° respectively.

This setup allows for an investigation into the influence of warm plasma injection on EMIC wave instability, with a particular focus on how varying ion temperature anisotropies and the cold-to-warm plasma ratio affect the wave growth rate. The derived dispersion relation and growth rate for parallel-propagating EMIC waves under these conditions are crucial for understanding the dynamics of wave-particle interactions in the Jovian magnetosphere.

Result and Discussion

To study the variation of various plasma parameters on growth rate with the effect of hot injection for ring distribution function in the presence of AC electric field, mathematical calculations have been performed.

Figure 1 shows the variation of growth rate (γ/ω_c) with the effect of hot injection on ion-cyclotron wave with respect to increasing $\tilde{k}$ for various values of AC frequency. Ring distribution function is assumed with the beam of energetic particles. Behavior of ion-cyclotron wave is shown in the graph by interaction of wave with hot injected particles in Jovian magnetosphere. AC frequency range has been taken from 2 Hz to 2.2 Hz. The growth rate (γ/ω_c) for υ = 2 Hz is 4.84211×10^{-06} at $\tilde{k}$=0.35, the growth rate (γ/ω_c) for υ = 2.1 Hz is 0.000011353024571591 at $\tilde{k}$=0.35 and for υ =2.2 Hz, the growth rate is γ/ω_c= 0.000025023536544779 at $\tilde{k}$=0.35. It is clearly seen that growth rate increases as the values of AC frequency increases. In **figure 2**, the variation of growth rate (γ/ω_c) with respect to increasing $\tilde{k}$ with the hot injection effect on EMIC for various values temperature anisotropy of cold ions has been plotted. For A_T =1.5, 2 and 2.5, the peak values are observed at $\tilde{k}$= 0.35, 0.35, 0.35 and the growth rates are γ/ω_c= $3.41842223973875\times10^{-06}$, 0.0000169021159039714 and 0.0000720765136280518 respectively. Thus, the relativistic growth rate increases as temperature anisotropy of cold plasma increases. Usually the temperature anisotropy of ions is greater than the electron's temperature anisotropy. Hence this condition leads to the wave growth reported by Kumari and Pandey[27].

Using **Figure 3**, variation of dimensionless growth rate in background plasma on EMIC wave in Jovian magnetosphere with respect to wave number $\tilde{k}$ for different values of number density n_0 at other fixed parameters is shown. For $n_0=4\times10^6$, the peak value of growth rate is γ/ω_c= 0.00023367 appears at $\tilde{k}$=0.4, for $n_0=5\times10^6$, growth rate is γ/ω_c= 0.002254457 at $\tilde{k}$=0.45 and as number density is increasing to $n_0=6\times10^6$, peak value γ/ω_c= 0.009471069 at $\tilde{k}$=0.5. So, as we increase number density n_0 from 4×10^6 to 6×10^6, growth rate increases, and peaks appear at same wave number $\tilde{k}$. **Figure 4,** shows the variation of growth rate (γ/ω_c) with the effect of propagation angle, θ_1 on ion-cyclotron wave with respect to increasing $\tilde{k}$. Propagation angle, θ_1 range has been taken from θ_1 =10° to 30°. The growth rate (γ/ω_c) for θ_1 =10° is

1.44723E-06 at $\tilde{k}$=0.30, the growth rate (γ/ω_c) for θ_1 =20° is 3.66646E-06 at $\tilde{k}$=0.35 and for θ_1 =30°, the growth rate is γ/ω_c= 1.7475E-06 at $\tilde{k}$=0.40. It is clearly seen that growth rate increases as the values of AC frequency increases.

Figure 5, shows the variation of growth rate (γ/ω_c) with the effect of background on ion-cyclotron wave with respect to increasing $\tilde{k}$ for various values of AC frequency with effect of magnetic field model. Ring distribution function is assumed with the beam of energetic particles. Behavior of ion-cyclotron wave is shown in the graph by interaction of wave with hot injected particles in Jovian magnetosphere. AC frequency range has been taken from 2 Hz to 2.2 Hz. The growth rate (γ/ω_c) for υ = 2 Hz is 6.3028E-09 at $\tilde{k}$=0.35, the growth rate (γ/ω_c) for υ = 2.1 Hz is 2.2927E-08 at $\tilde{k}$=0.35 and for υ =2.2 Hz, the growth rate is γ/ω_c= 7.49878E-08 at $\tilde{k}$=0.35. It is clearly seen that growth rate increases as the values of AC frequency increases. In **figure 6**, shows the effect of temperature anisotropy on growth rate with the effect of hot injected plasma with effect of magnetic field with respect to $\tilde{k}$of electromagnetic ion-cyclotron waves using ring distribution function in the Jovian magnetosphere. It can be seen that for A_T=1.5 the maxima occurs at $\tilde{k}$= 0.3 with γ/ω_c= 9.1863E-09, for A_T=2 the highest peak γ/ω_c= 4.24628E-08 occurs at $\tilde{k}$=0.3 and for A_T=2.5 the peak value γ/ω_c= 1.77683E-07 appears at $\tilde{k}$=0.3. It shows that growth increases for parallel propagation of EMIC wave in Jupiter's magnetosphere with increasing the magnitude of temperature anisotropy. **Figure 7,** shows the variation of growth rate (γ/ω_c) with the effect of propagation angle , θ_1 with the effect of magnetic field in ion-cyclotron wave with respect to increasing $\tilde{k}$. Propagation angle, θ_1 range has been taken from θ_1 =10° to 30°. The growth rate (γ/ω_c) for θ_1 =10° is 6.60128E-09 at $\tilde{k}$=0.35, the growth rate (γ/ω_c) for θ_1 =20° is 2.04613E-09at $\tilde{k}$=0.40 and for θ_1 =30°, the growth rate is γ/ω_c= 7.49878E-09 at $\tilde{k}$=0.40. It is clearly seen that growth rate increases as the values of AC frequency increases.

Figure 8 shows the effect of temperature anisotropy on growth rate with the effect of hot injected plasma with respect to $\tilde{k}$of electromagnetic ion-cyclotron waves using ring distribution function in the Jovian magnetosphere. It can be seen that for A_T=1.5 the maxima occurs at $\tilde{k}$= 0.55 with γ/ω_c= 0.525446451, for A_T=2 the highest peak γ/ω_c= 0.589756008 occurs at $\tilde{k}$=0.50 and for A_T=2.5 the peak value γ/ω_c= 0.658963625 appears at $\tilde{k}$=0.5. It shows that growth increases for parallel propagation of EMIC wave in Jupiter's magnetosphere with increasing the magnitude of temperature anisotropy. **Figure 9** shows the effect of relativistic factor on growth rate with the effect of hot injected plasma with respect to $\tilde{k}$of electromagnetic ion-cyclotron waves using ring distribution function in the Jovian magnetosphere. It can be seen that for β=0.7 the maxima occurs at $\tilde{k}$= 0.55 with γ/ω_c= 0.525446451, for β=0.8 the highest peak γ/ω_c= 0.531257736 occurs at $\tilde{k}$=0.50 and for β=0.9 the peak value γ/ω_c= 0.520711317 appears at $\tilde{k}$=0.45. It shows that growth rate shifts for higher value of wave number with decrease in the value of relativistic factor for parallel propagation of EMIC wave in Jupiter's magnetosphere with increasing the magnitude of relativistic factor. **Figure 10** shows the effect of number density ratio of electrons and ions on growth rate after injecting hot plasma with respect to $\tilde{k}$of EMIC waves using ring distribution function at Jupiter. It can be observe that for n_c/n_w = 1/10 the maxima occurs at $\tilde{k}$= 0.55 with γ/ω_c= 0.525446451, for n_c/n_w = 1/20 the highest peak γ/ω_c= 0.529429323 occurs at $\tilde{k}$=0.55 and for n_c/n_w = 1/30 the peak value γ/ω_c= 0.530342417 appears at $\tilde{k}$=0.55. It can be concluded that growth increases for parallel propagation of EMIC wave in Jupiter's magnetosphere as the magnitude increases. Thus, number density of electron does not affect the growth rate in the case of hot injection ion beam as[35] that dependence of dispersive properties of EMIC wave are on density and thermal plasma composition of ions. Using **Figure 11**, variation of dimensionless growth rate in background plasma with the effect of hot injection on EMIC wave with magnetic field model in Jovian magnetosphere with respect to wave number $\tilde{k}$ for different values of temperature anisotropy at other fixed parameters is shown. For A_T=1.75, the peak value of growth rate is γ/ω_c= 0.522046615 appears at $\tilde{k}$=0.55, for A_T=2, growth rate is γ/ω_c= 0.59197259 at $\tilde{k}$=0.55 and as A_T is increasing to 2.25, peak value γ/ω_c= 0.656393317 at $\tilde{k}$=0.5. So, as we increase temperature anisotropy from 1.5 to 2.5, growth rate increases, and peaks appear to shift towards a lower value of wave number $\tilde{k}$. **Figure 12** shows the effect of relativistic factor on growth rate with the effect of

hot injected plasma with respect to $\tilde{k}$of electromagnetic ion-cyclotron waves using ring distribution function in the Jovian magnetosphere in the presence of external magnetic field model. It can be seen that for β=0.7 the maxima occurs at $\tilde{k}$= 0.5 with γ/ω_c= 0.437003397, for β=0.8 the highest peak γ/ω_c= 0.48355298 occurs at $\tilde{k}$=0.5 and for β=0.9 the peak value γ/ω_c= 0.516484702 appears at $\tilde{k}$=0.5. It shows that growth increases for parallel propagation of EMIC wave in Jupiter's magnetosphere with increasing the magnitude of relativistic factor.

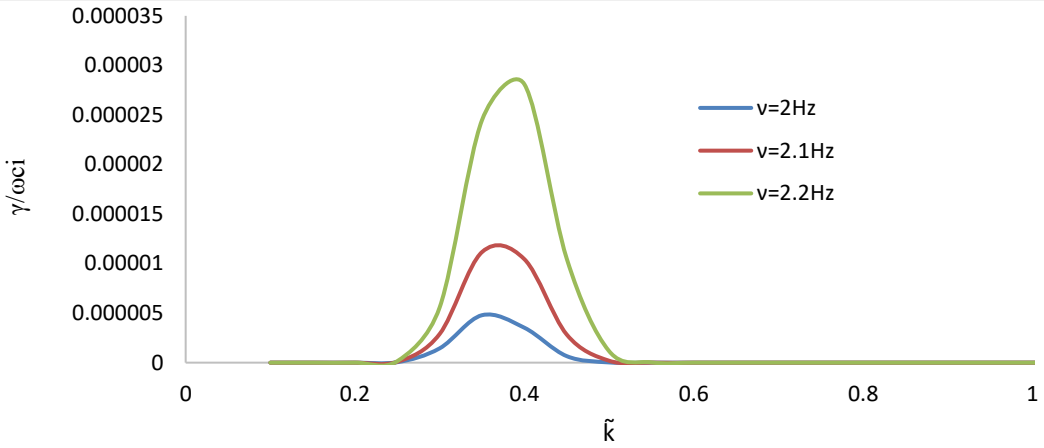

Fig.1: Variation of Growth Rate versus for different values of A.C frequency at n_0 = 3×10^6 m^{-3}, B_o=5.1x10^{-8}T, A_T=1.5, $K_BT_{||i}$=1 keV, $K_BT_{||ib}$=3 keV, $K_BT_{||e}$=200 eV, E_o=0.1 V/m, θ_1=10° and other fixed parameters of plasma at 17 R_J.

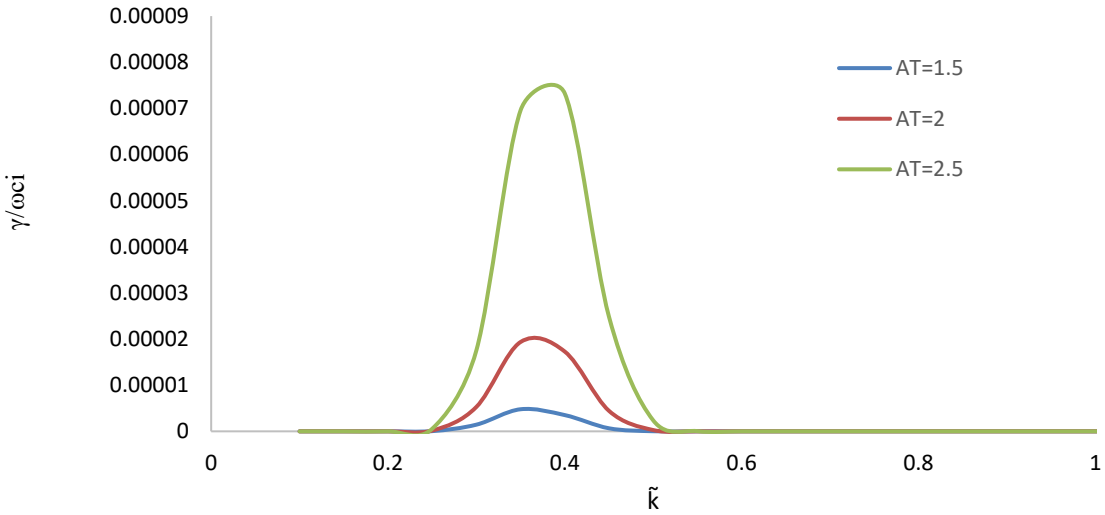

Fig.2: Variation of Growth Rate versus for different values of temperature anisotropy at n_0 = 3×10^6 m^{-3}, ν=2 Hz, $K_BT_{||i}$=1 keV, $K_BT_{||ib}$=3 keV, $K_BT_{||e}$=200 eV, B_o=5.1x10^{-8}T, E_o=0.1 V/m, θ_1=10° and other fixed parameters of plasma at 17 R_J.

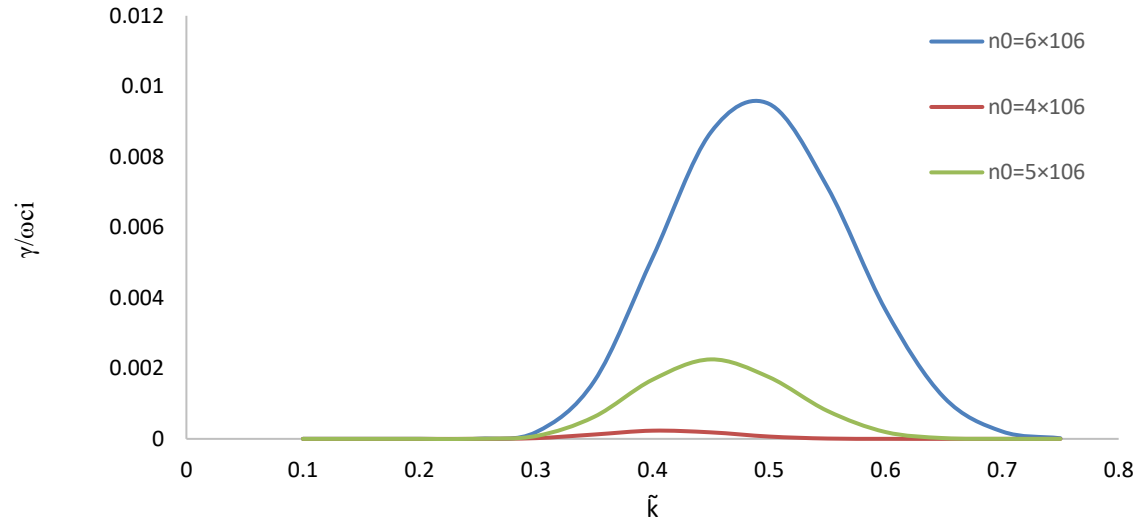

Fig.3: Variation of Growth Rate versus for different values of number density, n_0 at $n_0 = 3\times10^6$ m^{-3}, ν=2 Hz, $K_BT_{||i}$=1 keV, $K_BT_{||ib}$=3 keV, $K_BT_{||e}$=200 eV, B_o=5.1x10^{-8}T, E_o=0.1 V/m, θ_1=10° and other fixed parameters of plasma at 17 R_J.

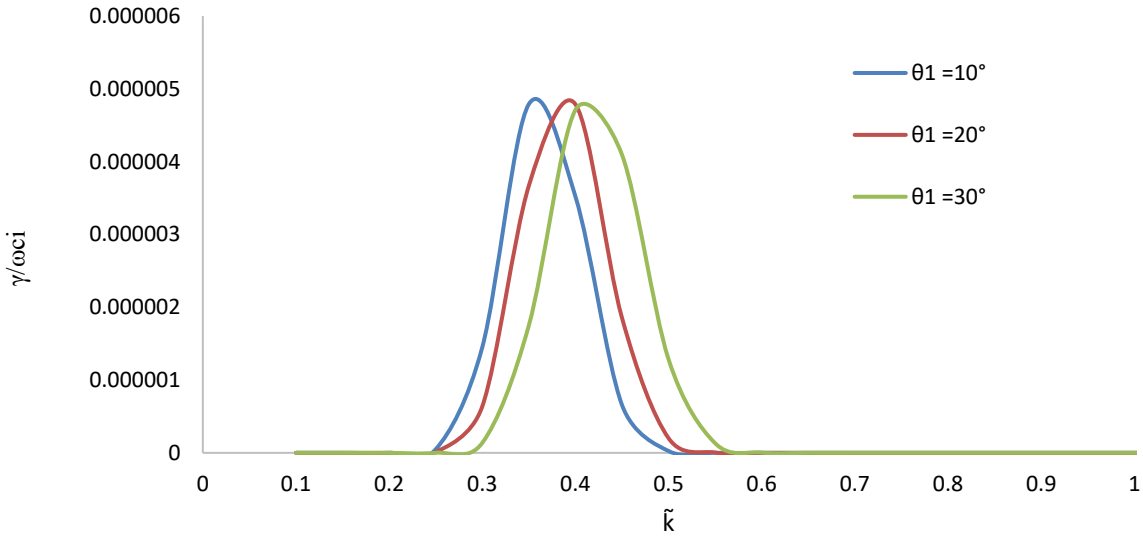

Fig.4: Variation of Growth Rate versus for different values of propogation angle,θ_1, n_0 at n_c/n_w=1/10, ν=2 Hz, $K_BT_{||i}$=1 keV, $K_BT_{||ib}$=3 keV, $K_BT_{||e}$=200 eV, B_o=5.1x10^{-8}T, E_o=0.1 V/m and other fixed parameters of plasma at 17 R_J.

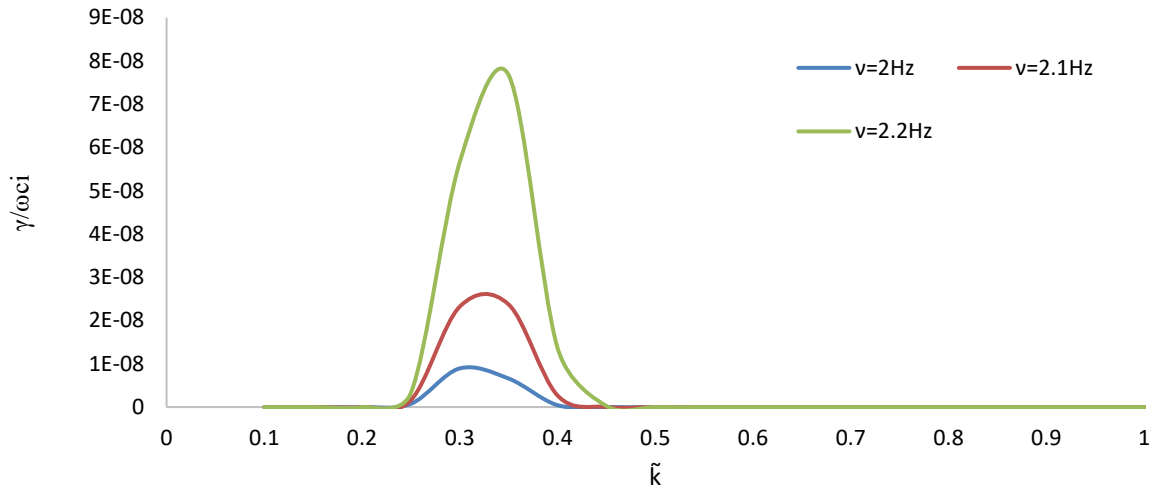

Fig.5: Variation of Growth Rate versus for different values of A.C frequency using magnetic field model at $n_0 = 3\times10^6$ m^{-3}, B_o=5.1x10^{-8}T, A_T=1.5, $K_BT_{||i}$=1 keV, $K_BT_{||ib}$=3 keV, $K_BT_{||e}$=200 eV, E_o=0.1 V/m, θ_1=10°, θ=10° and other fixed parameters of plasma at

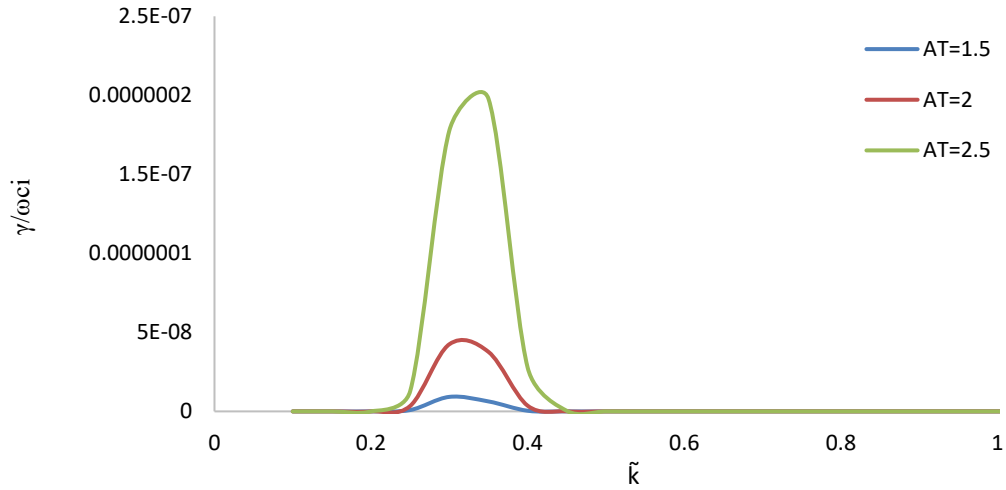

Fig.6: Variation of Growth Rate versus for different values of temperature anisotropy with magnetic field model at $n_0 = 3\times10^6$ m^{-3}, ν=2 Hz, $K_BT_{||i}$=1 keV, $K_BT_{||ib}$=3 keV, $K_BT_{||e}$=200 eV, B_o=5.1x10^{-8}T, E_o=0.1 V/m, θ_1=10°, θ=10° and other fixed parameters of p

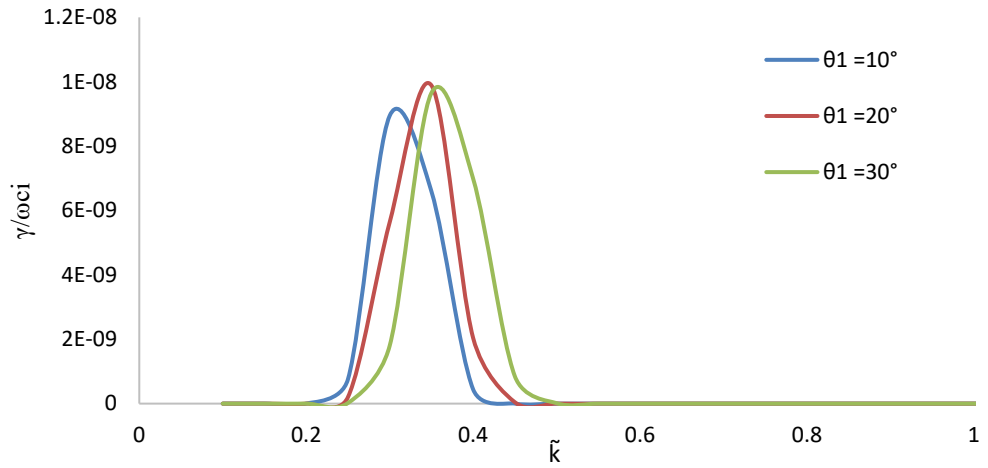

Fig.7: Variation of Growth Rate versus for different values of propogation angle,θ_1, with magnetic field model n_0 at n_c/n_w=1/10, ν=2 Hz, $K_BT_{||i}$=1 keV, $K_BT_{||ib}$=3 keV, $K_BT_{||e}$=200 eV, B_o=5.1x10^{-8}T, E_o=0.1 V/m and other fixed parameters of plasma at 17 R_J.

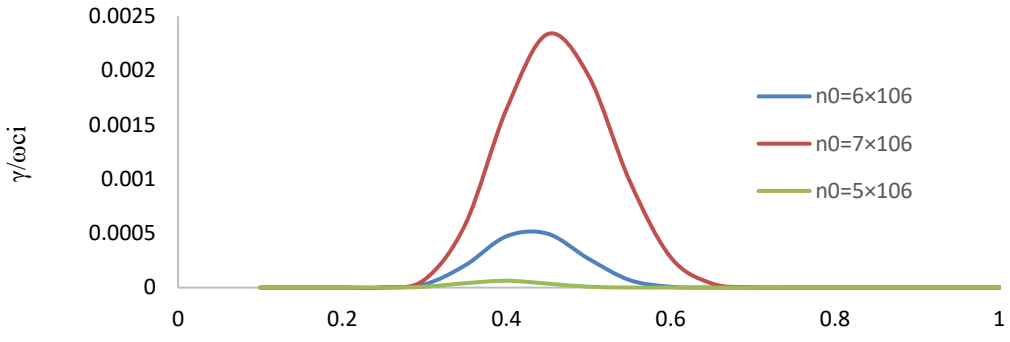

Fig.8: Variation of Growth Rate versus for different values of number density, n_0 at n_0= 3×10^6 m^{-3}, ν=2 Hz, $K_BT_{||i}$=1 keV, $K_BT_{||ib}$=3 keV, $K_BT_{||e}$=200 eV, B_o=5.1x10^{-8}T, E_o=0.1 V/m, θ_1=10° and other fixed parameters of plasma at 17 R_J.

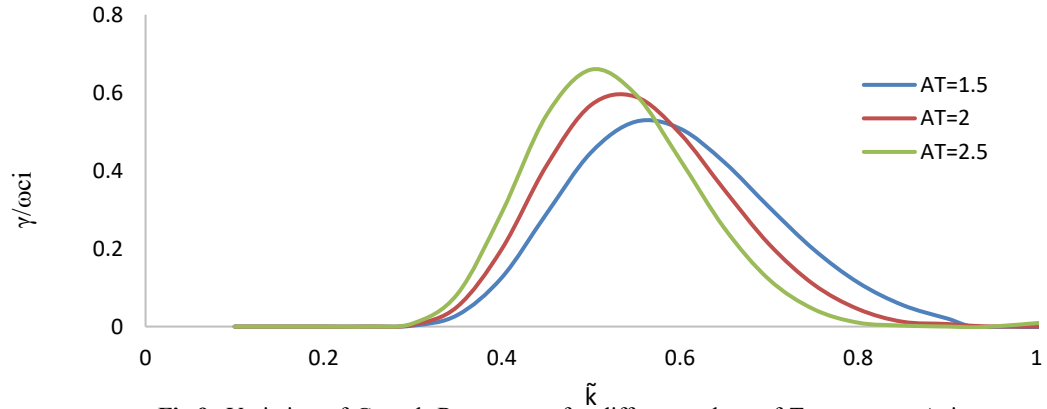

Fig.9: Variation of Growth Rate versus for different values of Temperature Anisotropy with beam at n_c/n_w=1/10, B_o=5.1x10^{-8}T, $K_BT_{||i}$=1 keV, $K_BT_{||ib}$=3 keV, $K_BT_{||e}$=200 eV, E_o=0.1 V/m, θ_1=10° and other fixed parameters of plasma at 17 R_J.

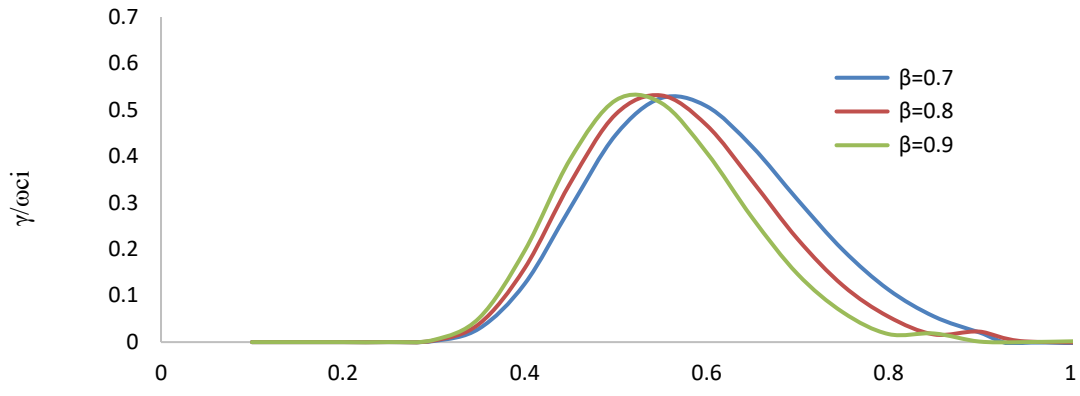

Fig.10: Variation of Growth Rate versus for different values of relativistic factor with beam at n_c/n_w=1/10, B_o=5.1x10^{-8}T, A_T=1.5, $K_BT_{||i}$=1 keV, $K_BT_{||ib}$=3 keV, $K_BT_{||e}$=200 eV, E_o=0.1 V/m, θ_1=10° and other fixed parameters of plasma at 17 R_J.

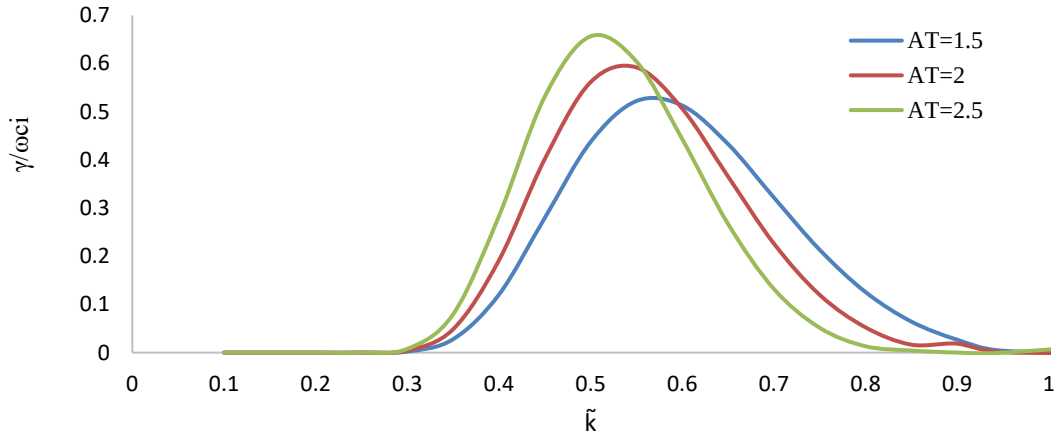

Fig.11: Variation of Growth Rate versus for different values of temperature anisotropy with beam with magnetic field model at n_c/n_w=1/10, ν=2 Hz, $K_BT_{||i}$=1 keV, $K_BT_{||ib}$=3 keV, $K_BT_{||e}$=200 eV, B_o=5.1x10^{-8}T, E_o=0.1 V/m, θ_1=10°, θ=10°and other fixed parameters

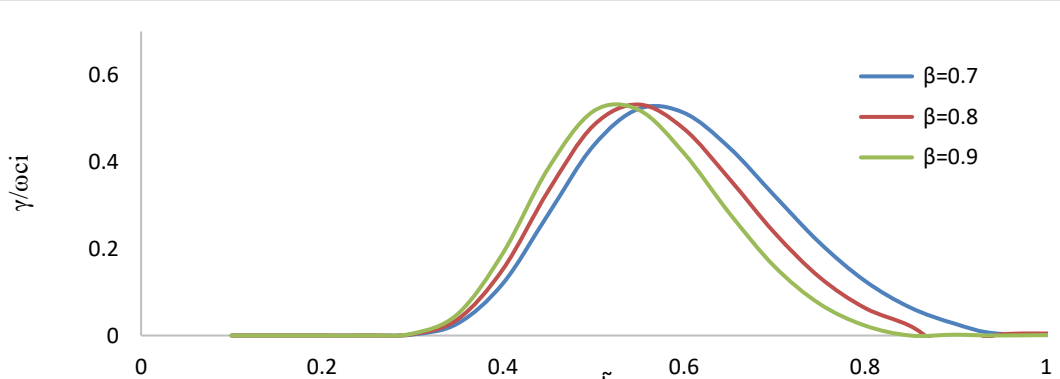

Fig.12: Variation of Growth Rate with relative to different values of relativistic factor with beam with magnetic field model at n_c/n_w=1/10, =2 Hz, A_T=2, B_o=5.1x10^{-8}T, $K_BT_{||i}$=1 keV, $K_BT_{||ib}$=3 keV, $K_BT_{||e}$=200 eV, E_o=0.1 V/m, θ_1=10°, θ=10°and other fixed p

Conclusion

This research examines the effects of hot injection on ring distribution in the magnetosphere of Jupiter at a radial distance of 17 RJ using parallel propagating electromagnetic ion-cyclotron waves in the presence of an AC electric field. The kinetic technique has been used to improve uniformity and efficiency. For the parametric investigation, the dispersion relation, true frequency, and growth rate have all been expressed in detail. Graphs have been produced in relation to wavenumber in order to examine plasma properties such as temperature anisotropy, AC frequency, etc. The findings indicate that ion-cyclotron waves increase at Jupiter. Following hot ion beam injection, growth rate rises as AC frequency rises and falls as temperature anisotropy rises from 1.5 to 2.5. Graphs demonstrate that for a given parameter, the peak emerges at the same wavenumber value.

Acknowledgement. We are thankful to SERB New Delhi for financial support and also thankful to Dr. Ashok K. Chauhan (Founder President, Amity University), Dr. Atul Chauhan (President, Amity University) and Dr. Balvinder Shukla (Vice Chancellor, Amity University) for their immense encouragement.

ORCID IDs

Garima Yadav ORCID iD-https:orcid.org/0009-0005-3239-599

B.S.Sharma ORCID iD-https:orcid.org/0000-0002-2327-9396

Ankita ORCID iD-https://orcid.org/0009-0009-2201-6453

References

1. Hanasz, J., Panchenko, M., de Feraudy, H., Schreiber, R., Mogilevsky, M.M., 2003. Occurrence distributions of the auroral kilometric radiation ordinary and extraordinary wave modes. J Geophys Res Space Phys Volume108, IssueA11, 1408 **https://doi.org/10.1029/2002JA009579**
2. Gendrin, R., 1975. Waves and wave-particle interactions in the magnetosphere: A review. Space Sci Rev vol 18, Nov. 1975, p. 145-200. 10.1007/BF00172533
3. Tsurutani, B.T., Smith, E.J., Anderson, R.R., Ogilvie, K.W., Scudder, J.D., Baker, D.N., Bame, S.J., 1982. Lion roars and nonoscillatory drift mirror waves in the magnetosheath. J Geophys Res Space Phys 87, 6060–6072. **https://doi.org/10.1029/JA087iA08p06060**
4. Kurth, W.S., Gurnett, D.A., 1991. Plasma waves in planetary magnetospheres. J Geophys Res Space Phys 96, 18977–18991. **https://doi.org/10.1029/91JA01819**
5. Livermore, P.W., Wu, L., Chen, L., de Ridder, S., 2024. Reconstructions of Jupiter's magnetic field using physics-informed neural networks. Mon Not R Astron Soc 533, 4058–4067. https://doi.org/10.1093/mnras/stae1928
6. Funke, B., López-Puertas, M., Bermejo-Pantaleón, D., García-Comas, M., Stiller, G.P., von Clarmann, T., Kiefer, M., Linden, A., 2010. Evidence for dynamical coupling from the lower atmosphere to the thermosphere during a major stratospheric warming. Geophys Res Lett 37. **https://doi.org/10.1029/2010GL043619**
7. Summers, D., Ma, C., Meredith, N.P., Horne, R.B., Thorne, R.M., Anderson, R.R., 2004. Modeling outer-zone relativistic electron response to whistler-mode chorus activity during substorms. J Atmos Sol Terr Phys 66, 133–146. https://doi.org/10.1016/j.jastp.2003.09.013
8. Bagenal, F., Delamere, P.A., 2011. Flow of mass and energy in the magnetospheres of Jupiter and Saturn. J Geophys Res Space Phys 116. **https://doi.org/10.1029/2010JA016294**
9. Kivelson, M.G., Khurana, K.K., 2002. Properties of the magnetic field in the Jovian magnetotail. J Geophys Res Space Phys Volume107, IssueA8**,** Page 23-9 **https://doi.org/10.1029/2001JA000249**
10. Kivelson, M.G., Southwood, D.J., 2005. Dynamical consequences of two modes of centrifugal instability in Jupiter's outer magnetosphere. J Geophys Res Space Phys 110. **https://doi.org/10.1029/2005JA011176**
11. Chen, F.F., 1984. Kinetic Theory, in: Introduction to Plasma Physics and

Controlled Fusion. Springer US, Boston, MA, pp. 225–285. https://doi.org/10.1007/978-1-4757-5595-4_7

12. Wei, J., Wang, G., Zuo, P., 2024. Study of the characteristics of electron firehose unstable conditions in the terrestrial magnetotail plasma sheet. Front Phys 12. https://doi.org/10.3389/fphy.2024.1446646
13. Loto'aniu, T.M., Fraser, B.J., Waters, C.L., 2005. Propagation of electromagnetic ion cyclotron wave energy in the magnetosphere. J Geophys Res Space Phys 110. **https://doi.org/10.1029/2004JA010816**
14. Lu, G., Goncharenko, L.P., Richmond, A.D., Roble, R.G., Aponte, N., 2008. A dayside ionospheric positive storm phase driven by neutral winds. J Geophys Res Space Phys 113. **https://doi.org/10.1029/2007JA012895**
15. Hobara, Y., Kanemaru, S., Hayakawa, M., Gurnett, D.A., 1997. On estimating the amplitude of Jovian whistlers observed by Voyager 1 and implications concerning lightning. J Geophys Res Space Phys 102, 7115–7125. **https://doi.org/10.1029/96JA03996**
16. Nichols, J.D., Achilleos, N., Cowley, S.W.H., 2015. A model of force balance in Jupiter's magnetodisc including hot plasma pressure anisotropy. J Geophys Res Space Phys 120. **https://doi.org/10.1002/2015JA021807**
17. Russell, C.T., 2001. The dynamics of planetary magnetospheres. Planet Space Sci 49, 1005–1030, **DOI:**10.1016/S0032-0633(01)00017-4
18. Chum Chen- Yi, Matthew W. Christensen, Graeme L. Stephens & John H. Seinfeld (2014) Satellite-based estimate of global aerosol–cloud radiative forcing by marine warm clouds,*Nature Geoscience* **volume 7**, pages643–646 **DOI:**10.1038/ngeo2214
19. Yoon, P.H., Lee, J., Hwang, J., Seough, J., Choe, G.S., 2019. Whistler Instability Driven by Electron Thermal Ring Distribution With Magnetospheric Application. J Geophys Res Space Phys 124, 5289–5301. **https://doi.org/10.1029/2019JA026687**
20. Artemyev, A. V., Demekhov, A.G., Zhang, X. -J., Angelopoulos, V., Mourenas, D., Fedorenko, Y. V., Maninnen, J., Tsai, E., Wilkins, C., Kasahara, S., Miyoshi, Y., Matsuoka, A., Kasahara, Y., Mitani, T., Yokota, S., Keika, K., Hori, T., Matsuda, S., Nakamura, S., Kitahara, M., Takashima, T., Shinohara, I., 2021. Role of Ducting in Relativistic Electron Loss by Whistler-Mode Wave Scattering. J Geophys Res Space Phys 126. **https://doi.org/10.1029/2021JA029851**
21. Jao C.-S. and L.-N. Hau (2018), Electrostatic solitons and Alfvén waves generated by streaming instability in electron-positron plasmasPhys. Rev. E 98,013203. https://doi.org/10.1103/PhysRevE.98.013203
22. Jao , C.-S. Jao *and* L.-N. Hau (2020), Electrostatic and electromagnetic waves driven by current free electron beam instability: Effects of positron, background composition, and ion-to-electron mass ratio AIP Advances 10, 075112. https://doi.org/10.1063/5.0016198
23. Ni, B., Huang, J., Ge, Y., Cui, J., Wei, Y., Gu, X., Fu, S., Xiang, Z., Zhao, Z., 2018. Radiation belt electron scattering by whistler-mode chorus in the Jovian magnetosphere: Importance of ambient and wave parameters. Earth and Planetary Physics 1, 1–14. **https://doi.org/10.26464/epp2018001**
24. Horne, R.B., Thorne, R.M., 1994. Convective instabilities of electromagnetic ion cyclotron waves in the outer magnetosphere. J Geophys Res Space Phys 99, 17259–17273. **https://doi.org/10.1029/94JA01259**
25. Mauk, B.H., Mitchell, D.G., McEntire, R.W., Paranicas, C.P., Roelof, E.C., Williams, D.J., Krimigis, S.M., Lagg, A., 2004. Energetic ion characteristics and neutral gas interactions in Jupiter's magnetosphere. J Geophys Res Space Phys

109. **https://doi.org/10.1029/2003JA010270**
26. Mauk, B.H., Saur, J., 2007. Equatorial electron beams and auroral structuring at Jupiter. J Geophys Res Space Phys 112. **https://doi.org/10.1029/2007JA012370**
27. Kumari, J., Pandey, R.S., 2019. Study of VLF wave with relativistic effect in Saturn magnetosphere in the presence of parallel A.C. electric field. Advances in Space Research 63, 2279–2289. 10.1016/j.asr.2018.12.013
28. Kumar, S., Singh, S.K., Gwal, A.K., 2007. Effect of upflowing field-aligned electron beams on the electron cyclotron waves in the auroral magnetosphere. Pramana 68, 611–622. https://doi.org/10.1007/s12043-007-0063-z
29. Kumari Jyoti and R.S. Pandey, 2018 "Whistler mode waves for ring distribution with A.C. electric field in inner magnetosphere of Saturn", Astrophysics and Space Sciences, Vol 363: 249. https://doi.org/10.1007/s10509-018-3466-z,
30. Pandey, R.S., Kaur, R., 2016. Analytical study of whistler mode waves in presence of parallel DC electric field for relativistic plasma in the magnetosphere of Uranus. Advances in Space Research 58, 1417–1424. https://doi.org/10.1016/j.asr.2016.06.002
31. Yadava Garima , B.S. Sharma , Ankita 2024 Generation of electromagnetic ion-cyclotron wave by hot injection of ion beam for ring distribution with electric field in Jovian magnetosphere, *East Eur. J. Phys. ,Accepted* .
32. Feldman W. C., Asbridg J. R., Bame S. J. and Montgomery M.D., (1973), On the Origin of Solar Wind Proton Thermal Anisotropy, *J. Geophys. Res.* , 78, 3697.
33. Agarwal, S., Pandey, R.S., Jeyaseelan, C., 2019. Exploring the effect of various plasma parameters on whistler mode growth rates in the Jovian magnetosphere. Astrophys Space Sci 364, 133 https://doi.org/10.1007/s10509-019-3623-z
34. Kivelson,M.G. and Khurana K.K.2002, Properties of the magnetic field in the Jovian magnetotail J Geophys Res Vol 107, Issue A8 **https://doi.org/10.1029/2001JA000249**
35. Misra, K.D., Pandey, R.S., 1995. Generation of whistler emissions by injection of hot electrons in the presence of a perpendicular Ac electric field. J Geophys Res Space Phys 100, 19405–19411. **https://doi.org/10.1029/95JA01083**